Nanomechanical Resonators Operating in the Radio Frequency Regime as Single Charge Detectors

R. H. Blick, A. Erbe. A. Tilke, H. Krömmer, L. Pescini, S. Manus, A. Kriele, J. P. Kotthaus

Center for NanoScience and Sektion Physik,
Ludwig-Maximilians-Universität, Geschwister-Scholl-Platz 1, D-80539 München

Summary: We present our recent work on nanomachined electromechanical resonators applied as mechanically flexible beams and tunneling contacts operating in the radio frequency regime. We will discuss how to build Au/Si beams of lengths varying from 1-4 μm and width down to only 80 nm. The resonators are machined out of single-crystal silicon-on-insulator (SOI) substrates. We will demonstrate how these nanometersize devices can be used to mechanically transfer only a few electrons. Furthermore, we will show how to apply them as charge detectors and how to drive the freely suspended beams into nonlinear response. This not only allows even more sensitive charge detection, but also opens up new possibilities for nonlinear dynamics in mechanical systems close to the quantum limit.

1 Introduction

When Leonardo da Vinci around 1500 first envisaged simple mechanical tools and even flying machines, like his famous helicopter [1], some of these were dreams becoming reality only centuries later. Nowadays, we are used to an almost infinite variety of mechanical devices and machines, yet with the advent of nanotechnology we are on the brink of the renaissance of mechanics on the nanometer scale.

A straight forward example of a classical mechanical device are old fashioned door bells, which apply simple electromechanical resonators to generate sound. A common design for such a bell is to integrate a clapper in between two electrodes, where one is then charged by a current. At a certain voltage the mechanical clapper is pulled towards one of the electrodes and charge can flow onto the metallic link. The clapper itself is then pulled back by the mechanical restoring force and delivers the acquired charge to the grounded electrode. Naturally, many different realizations of bells exist, but basically we can note that the combination of electrostatic and mechanical forces in such a bell lead to a resonant transport

of electrons. Since the electron's charge is quantized a bell can in principle be used to count single electrons, much in the same way as in Millikan's famous experiment with oil drops [2] or by using single-electron transistors [3, 4, 5, 6], and also at microwave frequencies [7]. Here, we demonstrate a new technique for counting electrons with a mechanical resonator, which is based on a mechanically flexible tunneling contact.

2 The Quantum Bell – Transferring Electrons Mechanically

In the case of macroscopic bells the granularity of the charge carriers is not observed, due to the large currents applied. In the present case the underlying idea is to scale down a classical bell in order to build a 'quantum bell' with which single electrons can be transferred. Naturally, there are some differences between a classical bell and our resonator: We rely on radio frequency electrostatic excitation of the clapper and not on a small magnet. Moreover, the clapper shown in the scanning electron microscope (SEM) micrograph of Fig. 1 has a size of only 1000 nm × 150 nm × 190 nm (length × width × thickness), leading to eigenfrequencies up to 400 MHz. However, regarding the fundamental similarities we find that electrons are transferred by a mechanically flexible contact. Besides reducing the size of the resonator, a quantum bell requires tunneling contacts in order to achieve tunneling of only a few electrons in each cycle of motion onto and off the clapper.

In these first measurements we want to focus on the demonstration of electron tunneling through the contacts at different resonance frequencies. Hence, the clapper is fully metallized and we operate the bell as a mechanical switch, where we drive the clapper at radio frequencies up to 100 MHz and measure the dc-current of only a few electrons tunneling each cycle through the clapper/drain contact. The sample was machined out of a single-crystal silicon-on-insulator (SOI) substrate by a combined dry- and wet-etch process. The SOI-substrate consists out of a 190 nm thick silicon layer, a 390 nm SiO_2 sacrificial layer and the semi-insulating Si wafer material. In a first step optical lithography was performed defining metallic gates and pads capable of supporting radio and microwave frequencies. In a second step we used electron-beam lithography to define the metallic nanostructure. The metal layers deposited on Si during lithography are a thin adhesion layer of Ni/Cr (1.5 nm), a covering Au-layer (50 nm), and an Al-etch mask (30 nm). A reactive-ion etch was then applied to mill down the silicon by 600 nm not covered with metal. Finally, the sample was etched in diluted HF, defining the suspended silicon layer with a thickness of 190 nm. The suspended quantum bell can be seen in Fig 1: drain (D) and source (S) tips function as tunneling contacts for the metallized Si-clapper (C) in the

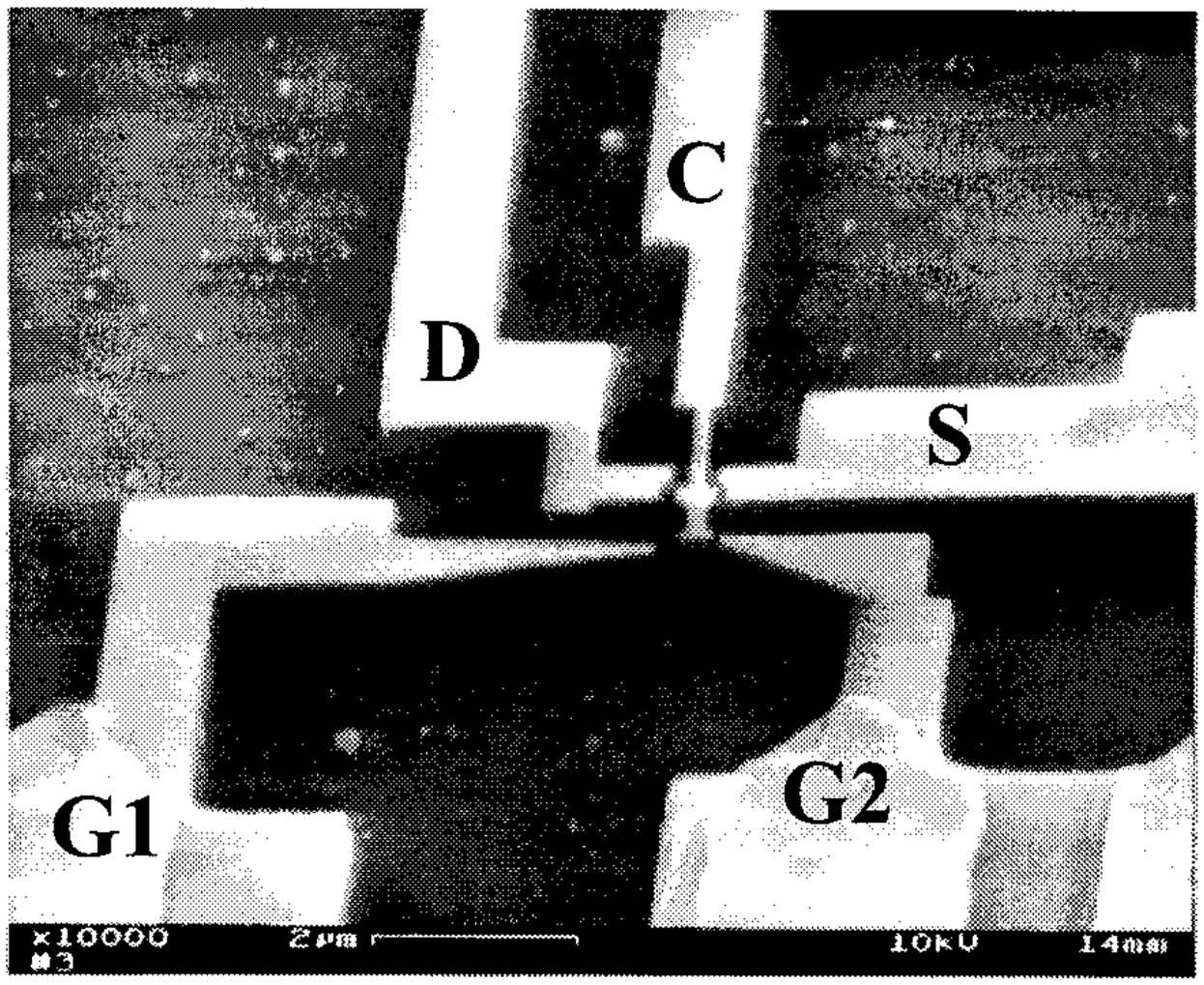

Figure 1 The quantum bell: A scanning electron beam micrograph of the suspended silicon structure: The clapper in the center is under-etched up to the second joint. The inset shows an electrical circuit diagram of the bell with drain (D), source (S), clapper (C) and gate contacts (#1 and #2). In the experiments shown we probe the current flowing through the clapper/drain contact. Radio frequencies are applied at gate contacts G#1 and G#2.

center.

In the present measurements the rf-modulation is applied to gates #1 and #2, while the source contact is grounded – the signal on gate #1 is phase shifted by $\phi = \pi$. We operate at frequencies up to some 100 MHz across the clapper electrode. Current then flows from the clapper to the drain contact and the dc-current is finally amplified. The sample is mounted in a standard sample holder allowing measurements in vacuum and at low temperatures. The obtained dc-IV-characteristic is shown in Fig. 2: At 300 K we find an exponential increase of the current with $V_{clapper/drain}$ when the clapper is pulled towards the drain contact around $V_{clapper/drain} \cong -1$ V. Electrons are then tunneling across the gap. Further biasing of the clapper finally leads to a metallic contact. The upper right inset shows the same characteristic measured at 4.2 K: Clearly the onset of the tunneling current occurs at larger bias voltage. The temperature dependence of the IV-characteristics can be explained by the enhanced Brownian motion and the reduced stiffness of the clapper at room temperature (no hysteresis is observed at 300 K).

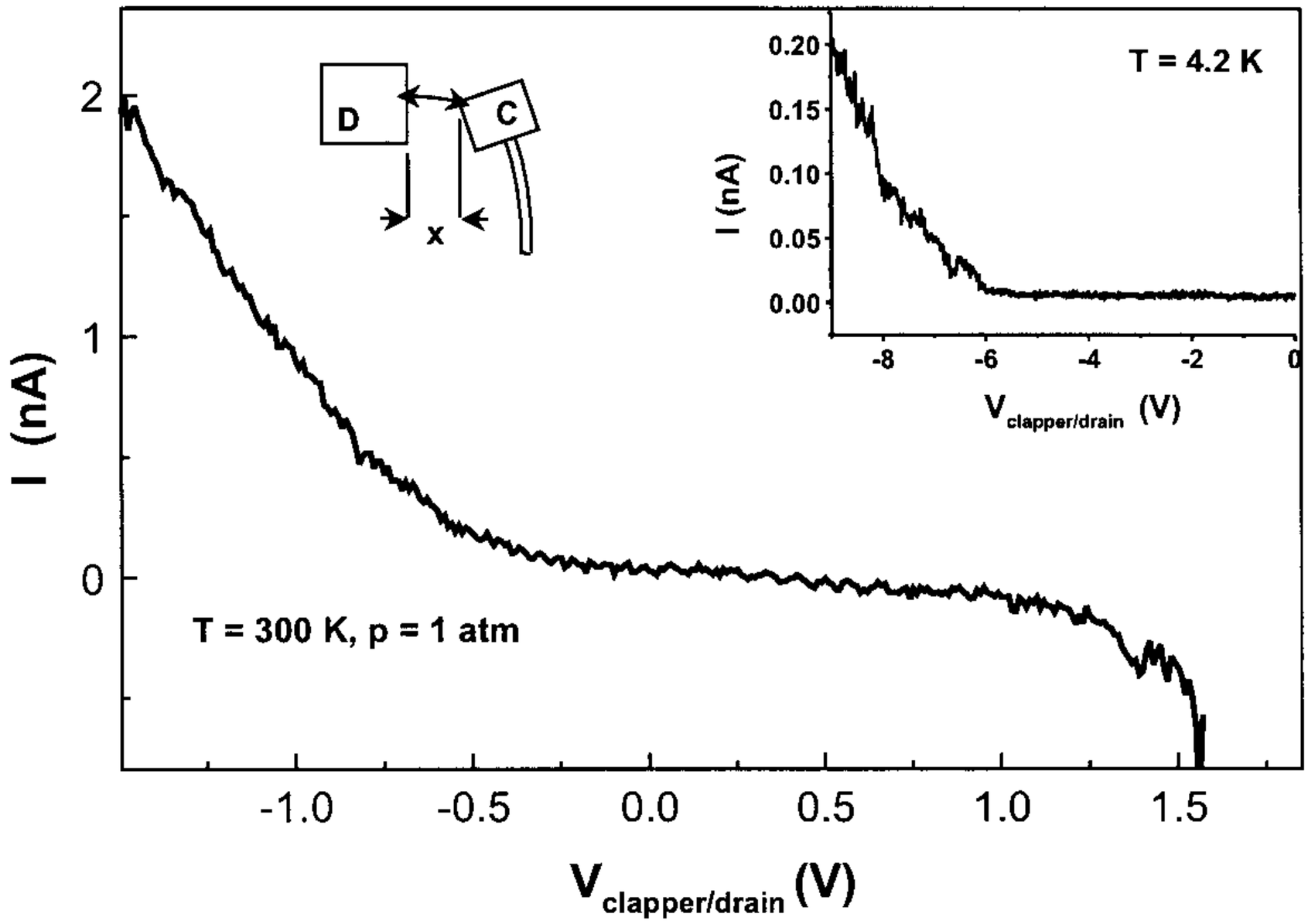

Figure 2 Static IV-characteristic of the mechanical clapper without radio frequency applied. Plotted is the dc-current as a function of bias voltage across the clapper/drain contact at $T = 300$ K. Inset shows the IV-characteristic at 4.2 K.

We have seen that the resistance of the contact (clapper/drain) depends exponentially on the tip displacement and hence on the distance to drain/source by $R(x(t)) = R_0 \exp(x(t)/\lambda)$. This can be adjusted by electrostatic tuning; λ is a material constant of the metallic electrodes defined by $\lambda^{-1} = \sqrt{(2m_e\Phi)}/\hbar$, with Φ being the work function and m_e the electron mass. This allows a mechanical variation of the RC-constant and hence the tunneling characteristics of the junction, which is not possible for common single electron transistor (SET) devices. By applying radio frequencies up to 100 MHz across gate #1 and the source contact, we finally realize the nanomechanical resonator. In order to verify appropriate rf-coupling we used a commercially available program (Sonnet Software, ver. 5.1, Liverpool, NY (USA), 1998). We find very effective coupling, which is only slightly attenuated towards 100 MHz. We estimate the capacitance of the clapper tip to drain contact to be on the order of $C \approx 25$ aF. This estimation is based on a method proposed by de Vries *et al.* [8] and on calculations with electromagnetic problem solvers (MAFIA, ver.3.20, 1993). Combining the capacitance and the tunneling resistance found in dc-measurements, we obtain an RC-constant of $\tau \sim 25$ aF $\times$ 1 GΩ = 25 nsec. Hence, the electrons are transferred one by one at a rate which can be approximated by the RC-constant. The values of 25 nsec corresponds to 40 MHz, which is the range of operation of our mechanical resonator. Hence, the mechanical motion leads to

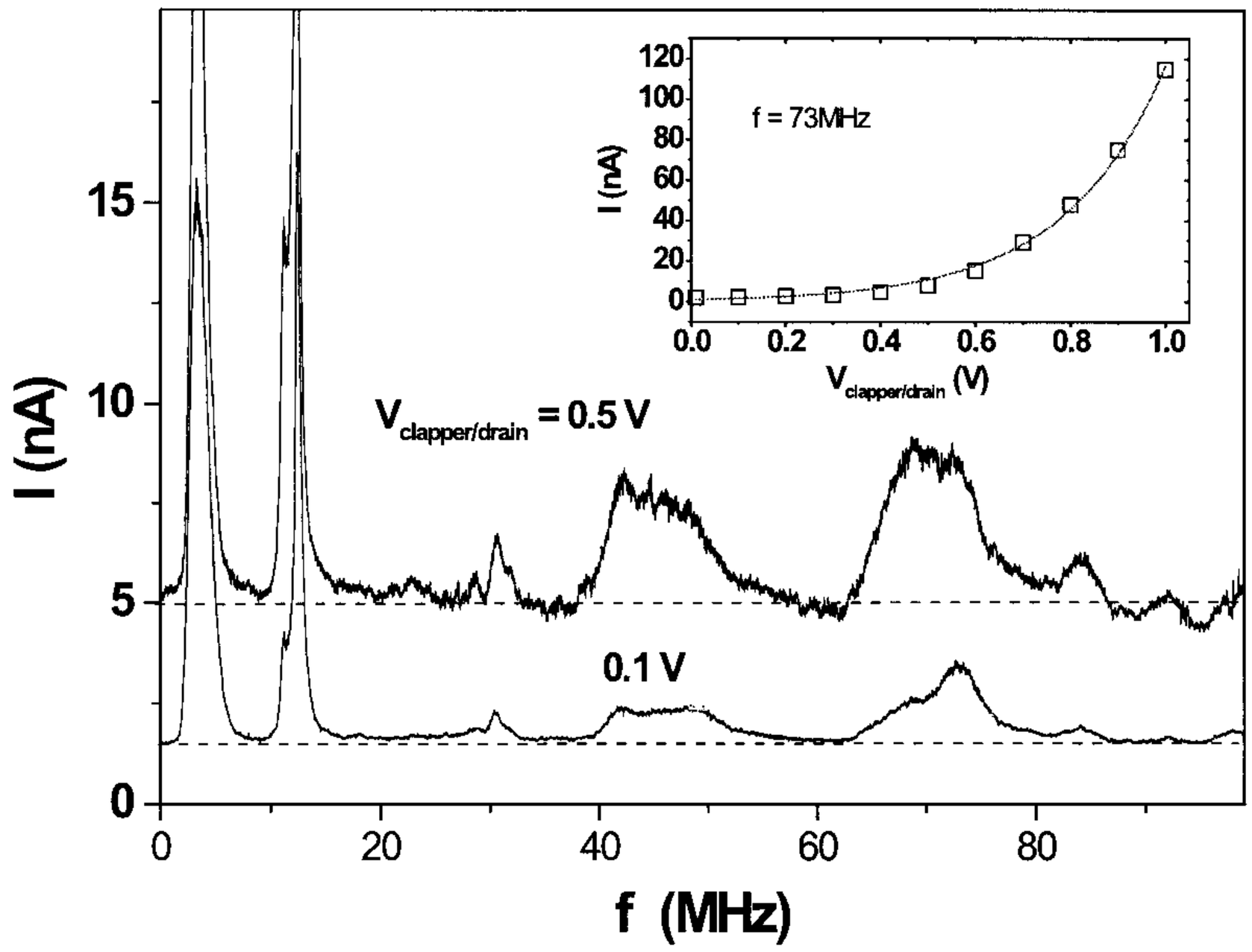

Figure 3 Resonance curves at different values of the dc-voltage bias across clapper/drain contact. The variation of the voltage bias results in an exponential increase of peak and background current. Inset: exponential behavior of peak current around 73 MHz – the solid line is an exponential fit to the data points (open boxes).

a modulation or 'chopping' of the electron tunneling rate. Electron tunneling is a discrete process, as exemplified by shot noise [9, 10]. Since we are able to modulate the resonator at this rate, we transfer only a small discrete number of electrons in each cycle of operation. In other words, the average current is given by $< I >=< q > f =< n > ef$, where $< n >$ is the average number of electrons being transferred at frequency f in each cycle.

A simulation of the mechanical properties of our resonator is performed with a software package (MCS PATRAN, ver. 6.2), allowing us to test the influence of shape and clamping points on the eigenmodes of the device. Since the Au-layer has almost the same thickness as the silicon supporting structure it is necessary to model a hybrid Au/Si-system. This is done by simply assuming two rigidly coupled bars with different spring constants ($\kappa_{Au} = 0.38$ N/m, $\kappa_{Si} = 46$ N/m – these values include geometrical factors). The resulting eigenfrequency spectrum

shows a strong resonant response between $f = 10$ and 100 MHz. It is obvious that the mass of the metallic layer on top reduces the attainable maximum frequency and the quality factor Q of our resonator ($Q = f/\delta f$). As expected, maximum strain is found at the clamping points, which further limits the performance (data not shown). Moreover, the specific shape of the resonator produces different eigenmodes, as will be shown in the measurements.

The rf-response of the resonator is presented in Fig. 3 – it is obtained at 300 K under He^4-gas pressure of 1 bar and an excitation amplitude of $V_{rf}^{pp} = \pm 5$ V: The different traces correspond to various dc-bias voltages on the clapper. As seen, we find a number of mechanical resonances with small quality factor Q of $\eta_1 \cong 100, \eta_2 \cong 30$, and $\eta_3 \cong 15$ where the complex resonance structure is a result of the geometry of the clapper. Here we assume that the mechanical resonator is not experiencing a back-action by the tunneling electrons. Applying the relation for the average dc-current $< I >=< n > ef$. In the low-frequency resonances up to 10^4 electrons are transferred in each cycle, while at 73 MHz we find a transfer rate of ~ 130 electrons at this amplitude of the driving voltage. The peak currents and the noise increase at larger bias voltages (0.1 V – 0.5 V). It can also be seen that the background conductance increases. The peak values themselves show an exponential increase of the current with $V_{clapper/drain}$, which is shown in detail in the inset for the peak at $f = 73$ MHz. Here the solid line is an exponential fit to the data points. From this exponential behavior of the peak current at 73 MHz shown in the inset of Fig. 3, we can estimate x, which gives a value for the distance between clapper and drain contacts at the maximum applied dc-voltage – we obtain $x_{max} \approx 5$ nm.

In a future setup of the experiment we will include a metallic island on the tip of the clapper, forming a metallic SET, in order to realize an electron shuttle mechanism, as proposed by Gorelik *et al.* [11]. A detailed theoretical description of this approach is already given by Weiss and Zwerger [12], indicating that such a mechanical single electron shuttle should operate up to temperatures of 1 K. The Coulomb repulsion in this case functions as an additional energy barrier for electrons to tunnel onto the island.

3 Charge Detection with a Nonlinear Mechanical Resonator

Another classical mechanical 'machine' is the guitar: Playing such an electrical guitar can be quite entertaining and technically difficult [13]. As everyone knows, the audible sounds of a guitar are generated by the clamped strings. Halving such a string the eigenfrequencies are increased by an octave. Scaling down the string to only some 100 nm yields frequencies in the radio frequency (RF) range. Recent work on such nanomechanical resonators [14, 15, 16] demonstrated their versatility, although not for musicians, but for applications in metrology. Integrating

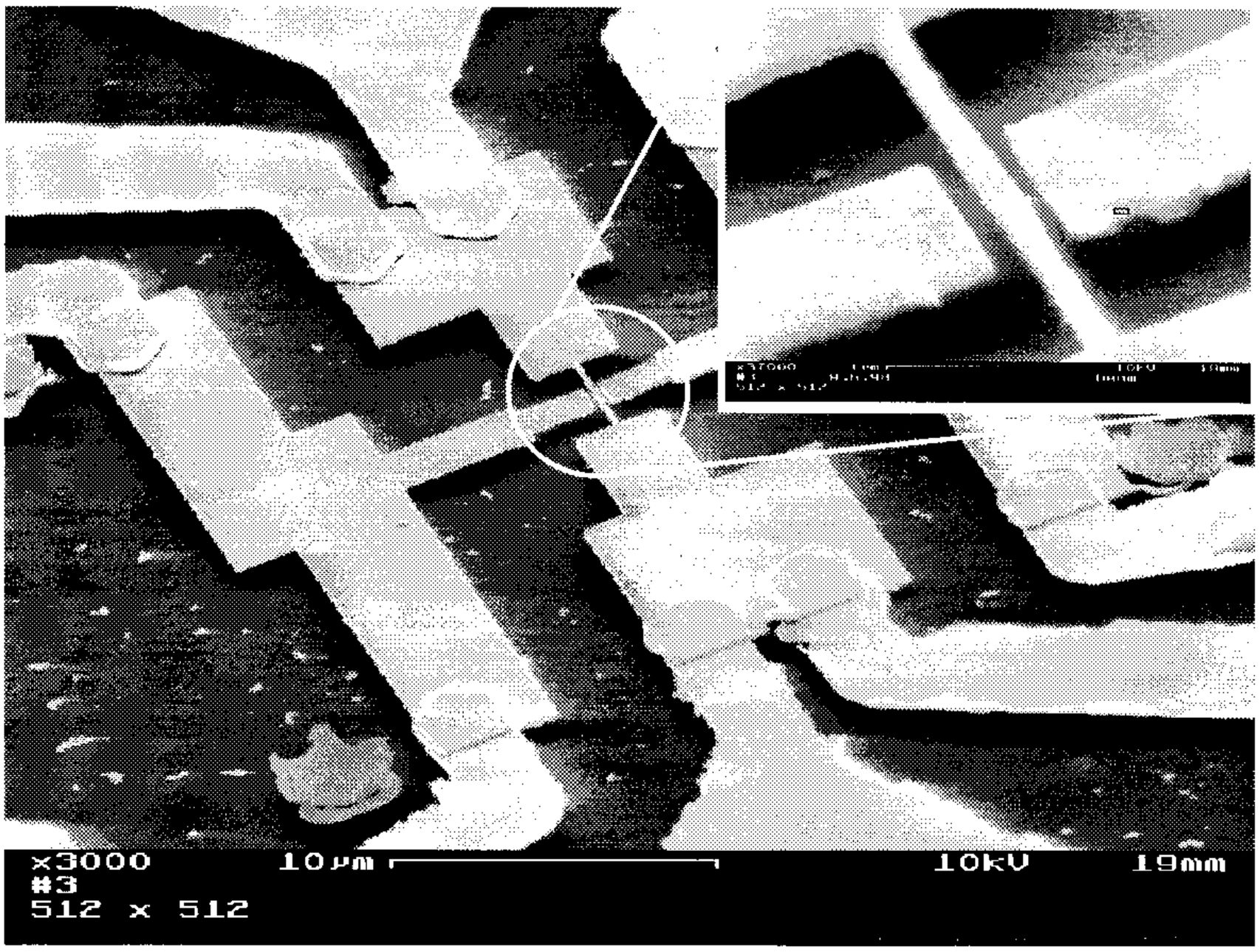

Figure 4 Micrograph of the nanomechanical resonator used in the experiment: The center gate couples to the resonator, machined out of Si with a 100 nm evaporated Au-layer.

mechanically flexible structures with single electron devices or two-dimensional electron gases [17] on the nanometer scale offers not only high speed of operation but also broad tunability of the tunneling contacts. This is of great interest regarding electrometry with single electron devices, which are currently limited to operating frequencies of 10 MHz and extremely low temperatures (< 10 mK). Applications of mechanical resonators in nonlinear oscillators [18] or parametric amplifiers [19] are of great importance for scanning probe measurements and accurate frequency counters or clocks in general.

In this second part of the work, we want to demonstrate how to observe nonlinear response of such nanomechanical resonators and how to apply these devices for charge detection. The resonators are operated in the RF regime with typical dimensions of only a few 100 nm in width and height. Applying a sufficiently large excitation amplitude the suspended beam shows a highly nonlinear response, which in turn allows extremely sensitive charge detection. The suspended resonator is shown in Fig. 4: The beam has a length of almost 3μm, a width of $w = 200$ nm and a height of $h = 250$ nm and is clamped on both sides. The gate contact couples capacitively to the resonator.

All measurements shown in this case were conducted at 4.2 K in a sample holder with a residual ^{4}He-gas pressure of about 10^{-2} bar. The sample was

mounted between interconnecting microstrip lines, designed to feed the circuit with frequencies up to 10 GHz, and then aligned in parallel with the externally applied magnetic field. The absolute resistance of the metal wire on top of the resonator was found to be 30 Ω, which results in a fairly well defined impedance matching of the whole circuit. In contrast to the electrostatic excitation of motion in case of the quantum bell, the beam is now set into motion by applying a high frequency electromagnetic excitation and ramping the magnetic field in plane. This results in an effective Lorentz force generated perpendicular to the sample surface. The response of the beam is finally probed with a spectrum analyzer, showing directly the electromagnetic power absorbed by the motion of the beam.

The capacitive coupling between beam and gate (see inset Fig. 4) is determined by numerical evaluation, as noted before. From these calculations we obtain a capacitive coupling between gate and beam in the linear regime of $C_{gb} \cong 220$ aF. The frequency shift $\delta\nu$ of the mechanical resonance is found to be

$$\delta\nu = \sqrt{\nu^2 - \frac{C''(0)}{2m_{eff}}V^2} - \nu \cong -\frac{C''(0)}{4m_{eff}\nu^2}V^2, \tag{3.1}$$

where m_{eff} is the beam's effective mass (in our case $\sim 4.3 \times 10^{-16}$ kg), V the applied gate voltage, and C'' represents the second derivative of the capacitance with respect to the spatial coordinate. This allows us to determine the relative charge δq on the closely connected gate with a high accuracy [20].

The nonlinearity found in the beam response (see Fig. 5) is caused by the variation of the restoring force at the clamping points [15] and can be modelled by adding a cubic term in the equation of motion of the beam [18]. Comparing the model derived by Greywall and Yurke [18] with our data we find excellent agreement.

Optimum operating conditions for electrometry are obtained by fixing the driving amplitude at the critical point as it is indicated in Fig. 5. The excitation power is levelled at -52.8 dBm and the magnetic field at 12 T. As seen in the inset the peak position varies as the square of the gate voltage applied. We achieve a sensitivity of $\Delta V/\sqrt{\Delta\nu} \cong 4.1 \times 10^{-2}$ V/$\sqrt{\text{Hz}}$. The slope at the critical point $dA/d\nu|_{\nu=\nu_c} \to \infty$ diverges resulting in extremely sensitive amplification. In the measurements presented we obtain a charge resolution at a finite bias on the gate ($V = \pm 4$ V) of $\sim 0.7 \times 10^2$ e/$\sqrt{\text{Hz}}$ limited by electronic noise. It is important to note the enhancement of sensitivity with increasing gate voltage (see inset of Fig. 5).

The accuracy of the measurement can even be more enhanced by determining the phase shift the mechanical resonance causes within the whole electrical circuit. For this measurement we modified our setup according to Ref. [14], i.e. including a mixer and a phase shifter. With this setup it was possible to obtain a sensitivity of $\sim 1.0 \times 10^{-1}$ e/$\sqrt{\text{Hz}}$. As before the operating point is adjusted in the transition region at the critical point.

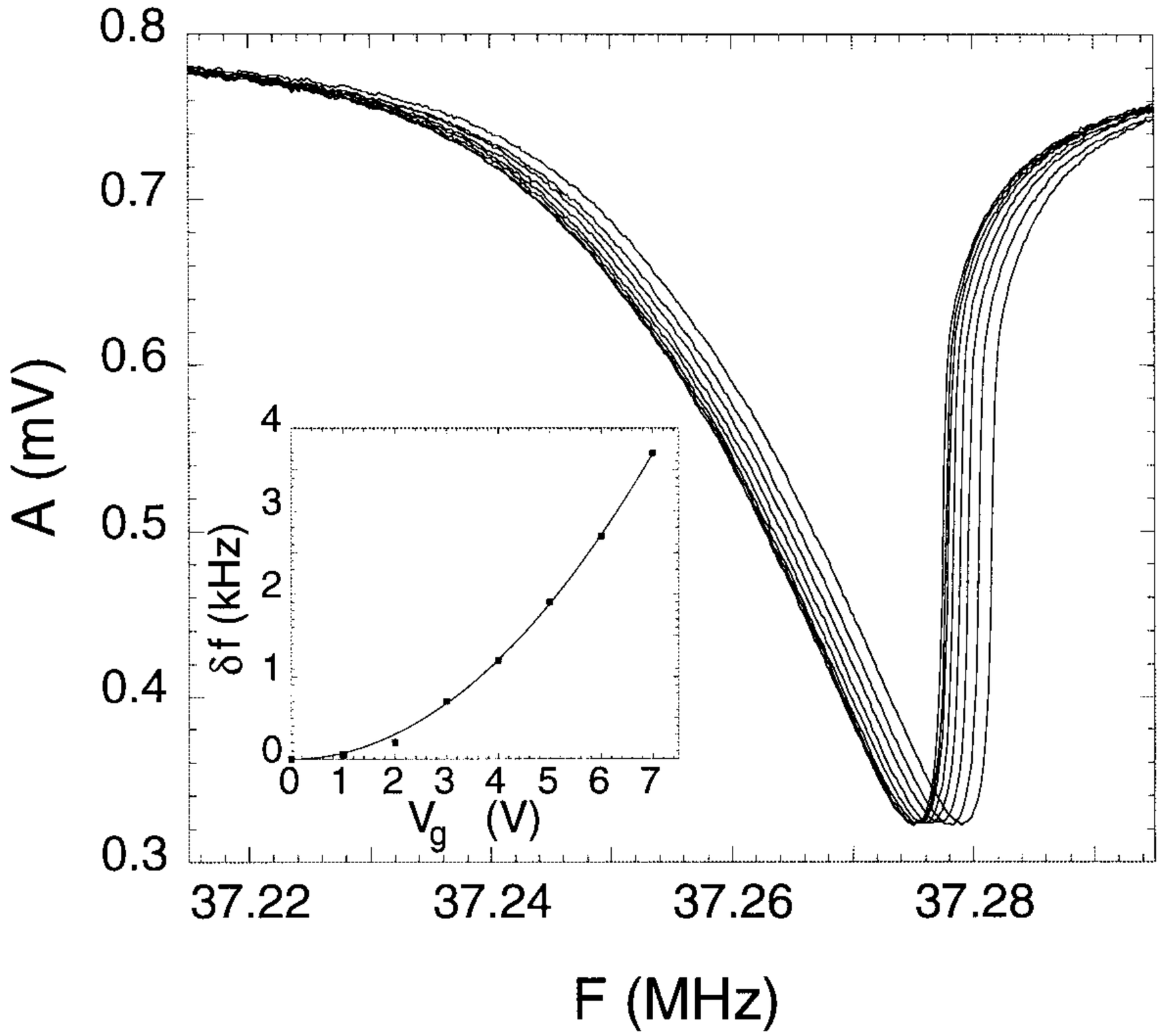

Figure 5 Operating the resonator in the transition region at $P_{exc} = -52.8$ dBm with maximum signal sensitivity. Resonance traces are shifted by an applied gate voltage. Note the shifting of the critical point when the gate voltage is varied (inset).

4 Summary and Outlook

In conclusion we demonstrated the operation of a variety of nanomechanical resonators. Our main focus is the accurate detection of single electron charges with the help of these mechanical devices. The main features are the high speed of operation and the increased sensitivity, due to the operation in the nonlinear regime. Furthermore, by scaling down a classical bell in size we have shown that a quantum bell can be built which rings in the ultrasonic frequency range.

5 Acknowledgements

We like to thank H. Lorenz, W. Zwerger, A. Wixforth, A. Lorke, and Ch. Weiss for extended discussions. This work was funded in part by the Bundesminis-

terium für Bildung, Wissenschaft, Forschung und Technologie (BMBF) and the Deutsche Forschungsgemeinschaft (DFG). The SOI-wafers used to machine the quantum bell were donated by Siemens Corp., Germany.

Bibliography

[1] Leonardo da Vinci, Codex Atlanticus (1500).

[2] R.A. Millikan, Phys. Rev. **32**, 349 (1911).

[3] T.A. Fulton and G.J. Dolan, Phys. Rev. Lett. **59**, 109 (1987).

[4] D.V. Averin and K.K. Likharev, J. Low Temp. Phys. **62**, 345 (1986).

[5] P. Lafarge, H. Pothier, E.R. Williams, D. Esteve, C. Urbina, and M.H. Devoret Z. Phys. B **85**, 327 (1991).

[6] M.W. Keller, J.M. Martinis, N.M. Zimmerman, and A.H. Steinbach, Appl. Phys. Lett. **69**, 1804 (1996).

[7] R.J. Schoelkopf, P. Wahlgren, A.A. Kozhevnikov, P. Delsing, D.E. Prober, Science **280**, 1238 (1998).

[8] D.K. de Vries, D. Stelmaszyk, and A.D. Wieck, J. Appl. Phys, **79**, 89 (1996).

[9] G. Schön, Phys. Rev. B **32**, 4469 (1985).

[10] H. Birk, M.J.M. de Jong, and C. Schönenberger, Phys. Rev. Lett. **75**, 1610 (1995).

[11] L.Y. Gorelik, A. Isacsson, M.V. Voinova, B. Kasemo, R.I. Shekhter, and M. Jonson Phys. Rev. Lett. **80**, 4526 (1998).

[12] Ch. Weiss and W. Zwerger, Europhys. Lett., in press (1999); cond-mat/9904149.

[13] 'Jimi Hendrix Experience – Radio One', James M. Hendrix (1967).

[14] A.N. Cleland and M.L. Roukes, Nature **392**, 160 (1998).

[15] A.N. Cleland and M.L. Roukes, Appl. Phys. Lett. **69**, 2653 (1996).

[16] A. Erbe, R.H. Blick, A. Tilke, A. Kriele, J.P. Kotthaus, Appl. Phys. Lett. **73**, 3751 (1998).

[17] R.H. Blick, M.L. Roukes, W. Wegscheider, and M. Bichler, Physica **B 249**, 784 (1998).

[18] D.S. Greywall, B. Yurke, P.A. Busch, A.N. Pargellis, and R.L. Willett, Phys. Rev. Lett. **72**, 2992 (1994); B. Yurke, D.S. Greywall, A.N. Paragellis, P.A. Busch, Phys. Rev. A **51**, 4211 (1995).

[19] D. Rugar and P. Grütter, Phys. Rev. Lett. **67**, 699 (1991).

[20] H. Krömmer, A. Erbe, A. Tilke, S. Manus, and R.H. Blick, submitted to Phys. Rev. Lett. (1999); H. Krömmer, diploma thesis, Ludwig-Maxmilians Universität München (1999).